C. R. Geoscience 350 (2018) 245–254

Contents lists available at ScienceDirect

Comptes Rendus Geoscience

www.sciencedirect.com

Petrology, Geochemistry

High-P amphibolite-facies metamorphism in the Adrar–Souttouf Metamafic Complex, Oulad Dlim Massif (West African Craton margin, Morocco)

Jose Francisco Molina [a,*], Fernando Bea [a], Pilar Montero [a], Faouziya Haissen [b], Francisco González-Lodeiro [c], Abdelattif Errami [d], Othman Sadki [d], Juan Antonio Moreno [a,e], Aitor Cambeses [a,f], Abdellah Mouttaqi [d]

[a] *Departamento de Mineralogía y Petrología, Universidad de Granada, Campus Fuentenueva, 18071 Granada, Spain*
[b] *LGAGE, Département de géologie, Faculté des sciences Ben Msik, Université Hassan-II, Casablanca, Morocco*
[c] *Departamento de Geodinámica, Universidad de Granada, Campus Fuentenueva, 18071 Granada, Spain*
[d] *Office national des hydrocarbures et des mines, 5, avenue Moulay-Hassan, Rabat, Morocco*
[e] *Centro de Investigaciones en Ciencias de la Tierra (CICTERRA), Consejo Nacional de Investigaciones Científicas y Técnicas, Facultad de Ciencias Exactas, Físicas y Naturales, Universidad Nacional de Córdoba, Av. Vélez Sarsfield 1611, Edificio de CICTERRA, X5016CGA, Córdoba, Argentina*
[f] *Institut de physique du globe de Paris, Sorbonne Paris Cité, CNRS, 75005 Paris, France*

ARTICLE INFO

Article history:
Received 27 January 2018
Accepted after revision 27 May 2018
Available online 11 July 2018

Handled by Isabelle Manighetti

Keywords:
Oulad Dlim Massif
Adrar–Souttouf Metamafic Complex
Garnet amphibolite
Metamorphism
Thermobarometry

ABSTRACT

The Oulad Dlim Massif represents the northern segment of the Mauritanide belt that thrusts over the western margin of the Reguibat Shield, north of the West African Craton (WAC). This belt includes various metamorphic units of Archean, Neoproterozoic and Palaeozoic ages that were stacked and thrust eastward during the Variscan orogeny. The core of the Oulad Dlim Massif comprises the Adrar–Souttouf Metamafic Complex that represents a large tectonic unit made of high-grade mafic rocks and vast exposures of amphibolites. A characterisation of the metamorphism in these amphibolites is essential to understand the relationships of the Oulad Dlim Massif with the southern segments of the Mauritanide belt and to provide constraints on the geodynamic evolution of the western margin of the WAC. Here we determine the *P–T* conditions of metamorphism of two samples of garnet amphibolites collected at the northernmost end of the Adrar–Souttouf Metamafic Complex. The samples show a main mineral assemblage of garnet + low-Ti
pargasite + oligoclase + phengite + epidote + quartz + rutile ± paragonite ± K-feldspar.
We calculated their *P–T* conditions using the amphibole–plagioclase NaSi–CaAl exchange thermometer, and the garnet–amphibole–plagioclase–quartz and the amphibole–plagioclase Si–Al partitioning barometers. The thermobarometric results indicate that this mineral assemblage was formed at high-P amphibolite-facies conditions at 650–700 °C and 10–13 kbar. The observed stability of paragonite and phengite reveals fluid-absent conditions or the presence of a fluid phase with reduced H_2O activity during the peak of metamorphism. We found no relicts of eclogite-facies mineral assemblage in the garnet amphibolites. This contrasts with the eclogite-facies metamorphism found due south in the Tarf Magneïna unit. This suggests that the northernmost end of the Adrar–Souttouf

* Corresponding author.
E-mail address: jfmolina@ugr.es (J.F. Molina).

https://doi.org/10.1016/j.crte.2018.05.005

Metamafic Complex may have been buried to shallower depths than the units further south, probably during the Variscan orogeny. However, precise absolute radiometric dating of the high-P amphibolite-facies metamorphism is required to confirm these findings.

1. Introduction

The Oulad Dlim Massif together with the Dhlou–Zemmour belt represent the northern extension of the Mauritanide belt that thrusts over the western margin of the Reguibat Shield in Morocco (Fig. 1) (e.g., Lécorché et al., 1991; Michard et al., 2008; Sougy, 1962a, 1962b; Villeneuve et al., 2006).

Recent geochemical and geochronological investigations provide a comprehensive framework of the Archean crust evolution of the Reguibat Shield (Montero et al., 2014) and the associated magmatism that constitutes the Western Reguibat Alkaline Province (WRAP; Bea et al., 2013, 2014, 2016; Montero et al., 2016, 2017). However, the structure and metamorphism of the Oulad Dlim Massif are still poorly understood (Michard et al., 2010) and various geological frameworks have recently been proposed (e.g., Gärtner et al., 2013, 2016; Montero et al., 2017; Villeneuve et al., 2015).

A detailed analysis of the metamorphism of the Oulad Dlim Massif is essential to determine its relationships with southern segments of the Mauritanide belt and to

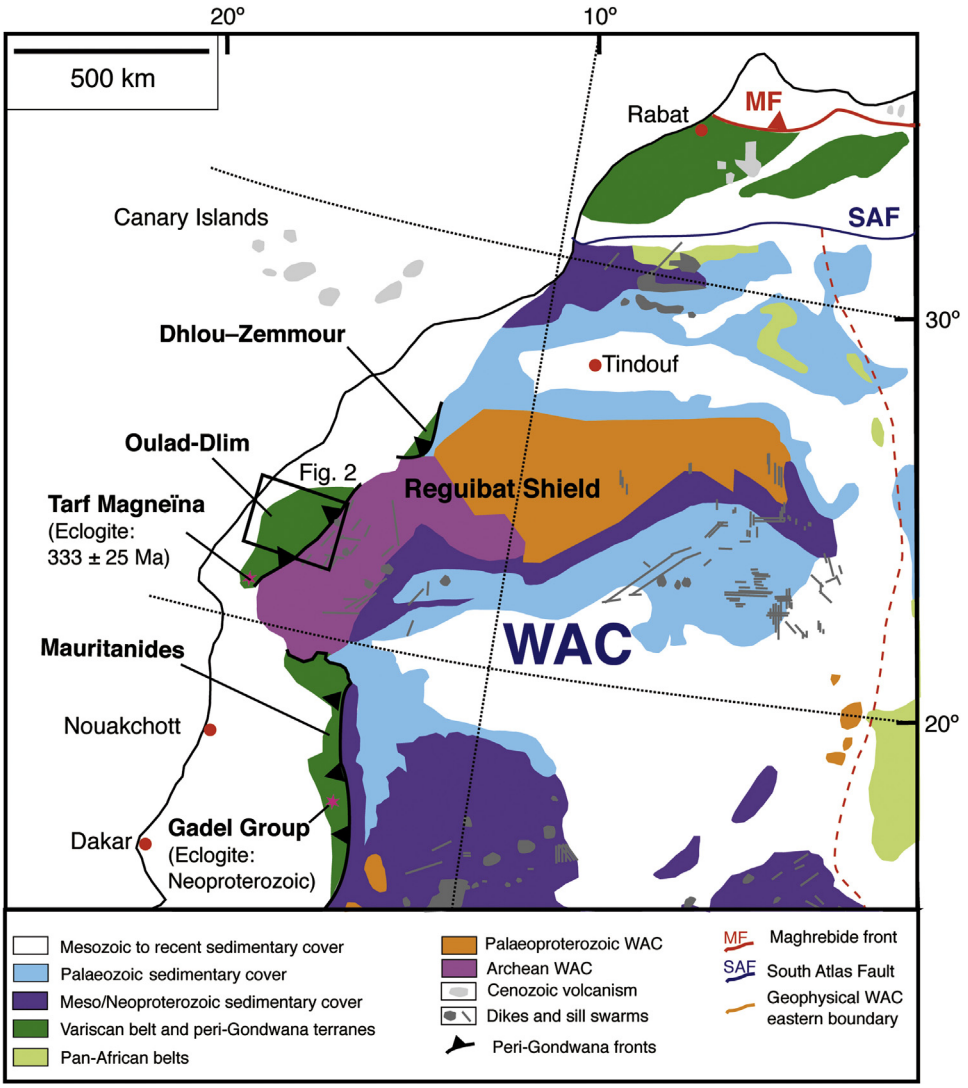

Fig. 1. General geological map of the West African Craton (after Ennih and Liégeois, 2008; Fabre, 2005; Michard et al., 2008, and references therein).

understand the Neoproterozoic to Palaeozoic geodynamic evolution at the western margin of the West African Craton (WAC). In this respect, the presence of eclogite-facies rocks of Variscan age in the Tarf Magneïna unit, just in the southernmost end of the Oulad Dlim Massif (Le Goff et al., 2001), and of Neoproterozoic age in Gadel Group from the Central Mauritanides (e.g., Caby and Kienast, 2009, and references therein) is a key for understanding the geodynamic framework (Fig. 1).

The metamorphism of the Oulad Dlim Massif is poorly known and eclogite-facies rocks have not yet been reported. A large tectonic unit, which includes high-grade mafic rocks, referred to as the Adrar–Souttouf Metamafic Complex (Montero et al., 2017), is exposed in the core of the Oulad Dlim Massif (Fig. 2). This metamorphic complex has vast exposures of amphibolites whose *P*–*T* conditions have not yet been established. To determine whether the eclogite-facies metamorphism extended to the north into the Adrar–Souttouf Metamafic Complex, we have studied the garnet amphibolites exposed in the northernmost end of the Adrar–Souttouf Metamafic Complex (Fig. 2). They indeed represent the most promising rock type to find relicts of eclogite-facies assemblages, for instance in the form of inclusions in garnet porphyroblasts. In this work, we describe field and textural relationships and estimate the *P*–*T* conditions of metamorphism registered in these amphibolites. The relationships with other high-P Mauritanide tectonic units are also discussed.

2. Geological setting and field relationships

The foreland of the Oulad Dlim Massif is formed by the Reguibat Shield and its thin sedimentary cover (Fig. 1). The Reguibat Shield consists of two domains, one Archean in the west and another Paleoproterozoic in the east, which were amalgamated during the 2.1–2.0 Ga Eburnean Orogeny (e.g., Schofield et al., 2006, and references therein). The Archean domain consists of granites, gneisses, migmatites, and greenstone belts intruded by undeformed magmatic rocks (Rjimati and Zemmouri, 2002). In the Awsard–Tichla zone, this domain comprises the tonalite–trondhjemite–granodiorite (TTG) Aghaylas Suite and the Tichla greenstone belt dated at 3.04–2.92 Ga and 3.03–3.01 Ga, respectively (Montero et al., 2014). They are intruded by the Awsard 2.46 Ga kalsilite syenites (Bea et al., 2013, 2014) and by a dense mafic dike swarm with probable Palaeoproterozoic to Mesoproterozoic ages (Dosso et al., 1979; Jessell et al., 2015; Youbi et al., 2013).

In the western border of the Reguibat Shield, the Archean domain is unconformably overlain by a discontinuous, narrow SW–NE band of Palaeozoic sedimentary rocks (Doloo–Esder–Tiznigaten units, Fig. 2) that begin with Upper Ordovician tilloids and arenites, followed by Silurian shales and Devonian shallow-water limestones (e.g., Michard et al., 2010, 2017, and references therein). This sedimentary succession is overlain by quartzites of the Tiznigaten unit (Rjimati and Zemmouri, 2002) that contains 510 Ma detrital zircons (Villeneuve et al., 2015). The Doloo–Esder–Tiznigaten units represent the detachment sole of the Oulad Dlim nappes in the Awsard area, as evidenced by intense shearing and development of tight, upright or east-verging folds (Michard et al., 2008, 2010; Rjimati and Zemmouri, 2002; Rjimati et al., 2011). In the Tichla area, the Oulad Dlim nappes thrust directly over the Archean basement (Fig. 2).

To the west, the Doloo–Esder–Tiznigaten units are thrust by the Oulad Dlim high-grade metamorphic units (Fig. 2). The Oulad Dlim Massif is interpreted as a nappe

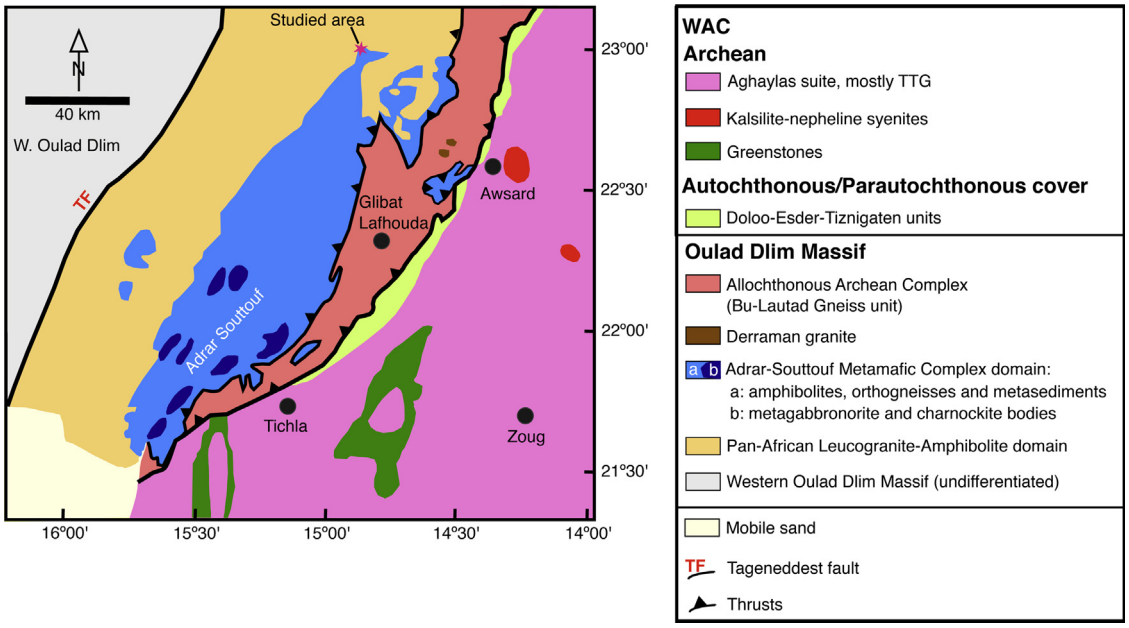

Fig. 2. Schematic geological map of the Oulad Dlim domain (after Montero et al., 2017).

stack of allochthonous metamorphic units affected by intense shearing of probable Variscan age (Michard et al., 2008, 2010; Rjimati et al., 2011; Sougy, 1962a, 1962b). The main tectonic units of the Oulad Dlim Massif located to the east of the Tageneddest fault as established in Montero et al. (2017) are displayed in the geological map of Fig. 2. The Oulad Dlim lowest unit corresponds to a large allochthonous Archean domain that was labelled the Bu-Lautad Gneiss unit (Montero et al., 2017). This Archean complex comprises a wide band, named the Bu-Lautad series by Arribas (1968), of felsic gneisses (3.0–3.1 Ga, Bea et al., 2016; SHRIMP U–Pb zircon dating) interlayered with high-grade metapelites, quartzites, marbles and, amphibolites, which is intruded by the 1.85 Ga Gleibat Lafhouda carbonatites in the south (Montero et al., 2016). This rock series is overlain by the low-grade Laglat micaschists with the youngest detrital zircons showing Neoarchean ages and by the 525 Ma Derraman riebeckite–aegyrine granitic gneisses (Bea et al., 2016; SHRIMP U–Pb zircon geochronology).

The Bu-Lautad Gneiss unit is thrust to the west by the Adrar–Souttouf Metamafic Complex, which contains one of the largest exposures of hyperstene-bearing rocks known in the Earth. This complex consists of intercalations of medium- to high-grade amphibolites, orthogneisses, marbles, and calc-silicate rocks with hundred metre- to kilometre-scale bodies of mafic granulites and charnockites (Arribas, 1968). The mafic granulite bodies consist of layered granoblastic metagabbronorites that are strongly mylonitized at their borders. The general orientation of the foliation varies from N 70–80°E dipping ca. 30°NW to N 0–50°E with steep dip. The mafic protoliths have been dated at 605–635 Ma by LA–ICPMS U–Pb zircon geochronology (Gärtner et al., 2016); SHRIMP U–Pb zircon dating confirms these ages, but also reveals that the protoliths are progressively younger to the west (Montero et al., 2017). The age of the high-grade metamorphism is unknown, being generally accepted to be pre-Variscan (e.g., Bea et al., 2016; Le Goff et al., 2001; Villeneuve et al., 2006).

The Pan-African Leucogranite–Amphibolite domain is exposed to the west of the Adrar–Souttouf Metamafic Complex via a non-tectonic contact. This domain consists of a bimodal series of dominant, strongly deformed, leucogranitic gneisses, and subordinate amphibolites. Both leucogranitic gneisses and amphibolites present Ediacaran crystallisation ages that are slightly younger than those obtained for the mafic rocks from the Adrar–Souttouf Metamafic Complex (Montero et al., 2017; SHRIMP U–Pb zircon geochronology). The leucogranite–amphibolite bimodal series abruptly terminates against the SSW–NNE-trending Tageneddest normal fault in its western border.

3. Samples and methods

The area investigated in this work represents a small outcrop (ca. 5 km^2) of garnet amphibolites interlayered with Mg-chlorite amphibolites partially covered with mobile sands (Fig. 3A and B), which is located in the northernmost end of the Adrar–Souttouf Metamafic Complex, along the Dakhla–Awsard road (ca. 22°58′35″N 14°47′49″W, Fig. 2). The main foliation in the studied area is rotated with respect to the regional orientation, striking N100–110°E and dipping 50–60° SW. The amphibolites are in close association with garnet-bearing felsic orthogneisses with phengite and biotite.

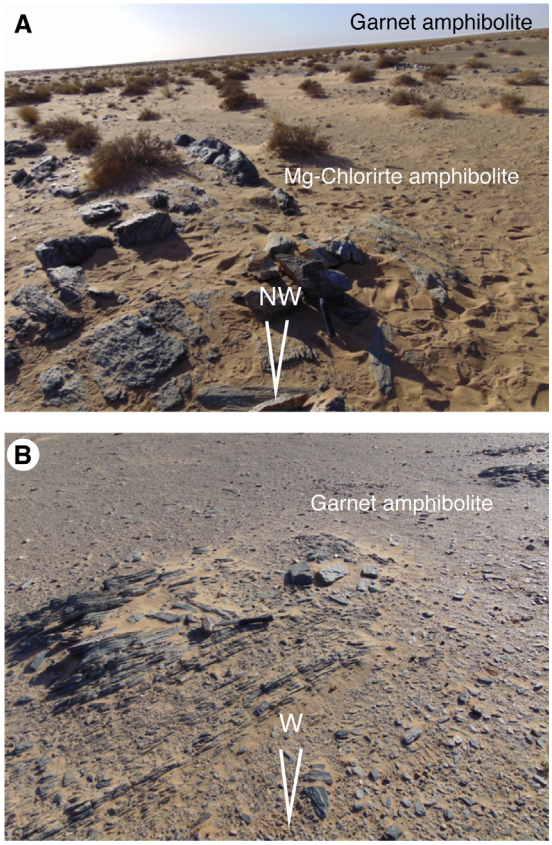

Fig. 3. Field relationships in the northernmost end of the Adrar–Souttouf Metamafic Complex. A. Intercalations of garnet amphibolites and Mg-chlorite amphibolites in the Adrar–Souttouf Metamafic Complex. B. Close-up of garnet amphibolite, showing a penetrative foliation.

For this work, we have studied seven samples of amphibolites from the Adrar–Souttouf Metamafic Complex. Two samples of garnet amphibolite were selected for textural, phase relationship, and mineral composition analyses: REG-100A and REG-100B.

Minerals were analysed by wavelength dispersive spectrometry (WDS) using a CAMECA SX100 electron microprobe at the "Centro de Instrumentación Científica" (CIC, University of Granada, Spain) using natural and synthetic standards. The accelerating voltage was 20 kV and the beam current was 20 nA. The precision was close to ± 4% for an analyte concentration of 1 wt.%. The mineral compositions were also determined by energy-dispersive X-ray (EDX) microanalysis on a ZEISS EVO-10 scanning electron microscope operated at 15 kV at the CIC, using natural mineral standards.

Selected mineral compositions are listed in Table 1 in the electronic Supplementary Material. The Fe^{3+}/Fe_T ratio

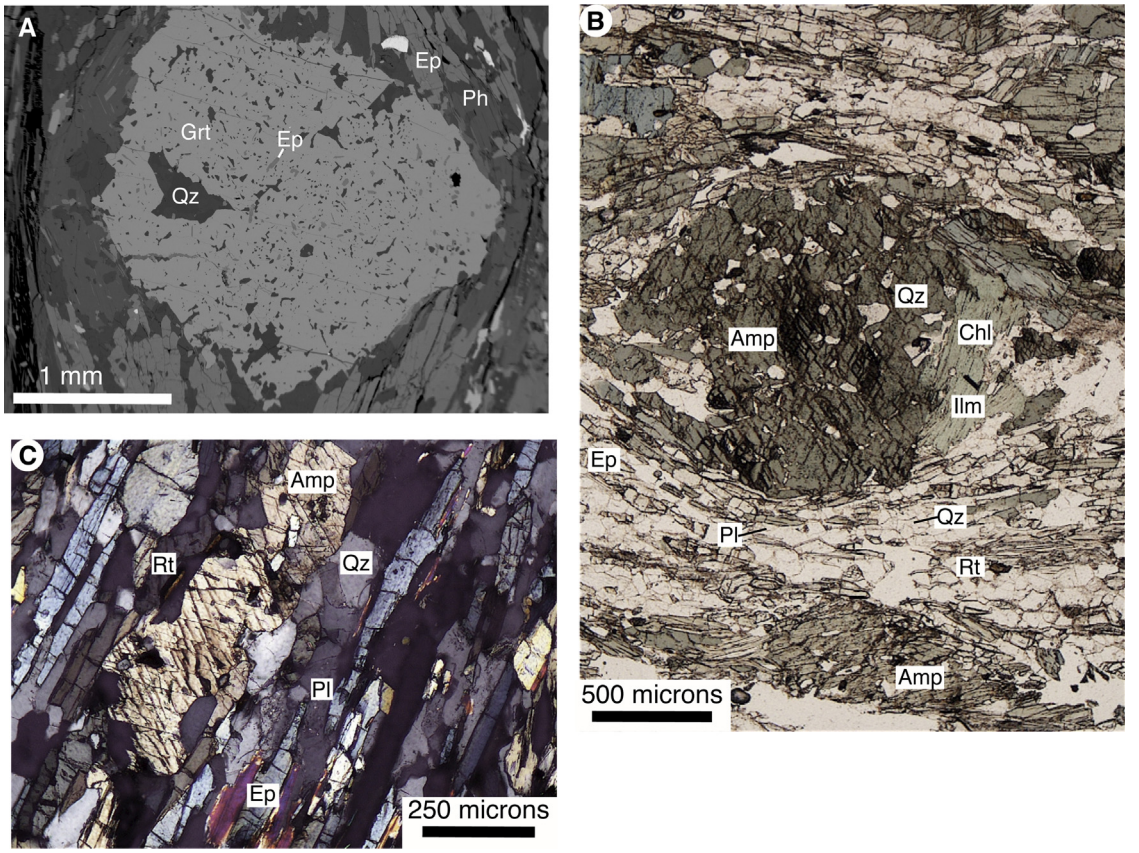

Fig. 4. Textural relationships in garnet amphibolites. A. Back-scattered electron (BSE) image of pre-kinematic poikiloblast of garnet with abundant inclusions of epidote and quartz. B. Photomicrograph of pre-kinematic poikiloblast of amphibole with abundant inclusions of quartz. Note medium-grained syn-kinematic poikiloblasts of amphibole with an internal foliation defined by the alignment of inclusions of quartz and epidote that is continuous with the external one. Plane-polarized light. C. Photomicrograph of the foliated rock matrix consisting of nematoblastic aggregates of amphibole, epidote and rutile, and granoblastic aggregates of plagioclase and quartz. Cross-polarized light. Mineral abbreviations after Whitney and Evans (2010).

in amphibole (normalisation to 23 O) and garnet (normalisation to 12 O) was calculated by charge balances and stoichiometric constraints; for the amphibole formula, the method presented in appendix A from Dale et al. (2005) was used, assuming OH + Cl + F = 2 atoms per formula unit, apfu. Mineral formulas for white micas were calculated assuming total Fe as Fe^{2+} (OH + Cl + F = 2 apfu; normalisation to 11 O), whereas for epidote (normalisation to 12.5 O) total Fe as Fe^{3+} was considered.

4. Results

4.1. Petrography

The garnet amphibolites present the amphibolite-facies mineral assemblage: garnet + low-Ti pargasite + oligoclase + phengite + epidote + quartz + rutile ± paragonite ± K-feldspar (called hereafter Grt–Prg–Pl mineral assemblage; mineral abbreviations after Whitney and Evans, 2010).

These rocks show an inequigranular fabric with scarce, coarse-grained pre-kinematic poikiloblasts of garnet and amphibole, with abundant, randomly distributed, inclusions of epidote and quartz (Fig. 4A, B). The rock matrix presents a penetrative foliation defined by medium-grained lepido-nematoblastic aggregates of amphibole, epidote, white mica and rutile, and granoblastic aggregates of plagioclase and quartz (Fig. 4C). Medium-grained syn-kinematic poikiloblasts of amphibole are also present, which show an internal foliation defined by an alignment of quartz and epidote inclusions that is continuous with the external one (Fig. 4B).

No reaction relationships are observed at the interface between poikiloblasts, both garnet and amphibole, and matrix minerals suggesting equilibrium relationships. Matrix minerals show abundant triple junctions, whereas evidence of intracrystalline strain is only observed in some quartz grains. These textural relationships point to an important post-kinematic recrystallization of matrix minerals. Neither relicts of omphacite nor its pseudomorphs were found, which makes unlikely the achievement of eclogite-facies conditions in the earlier metamorphic stages.

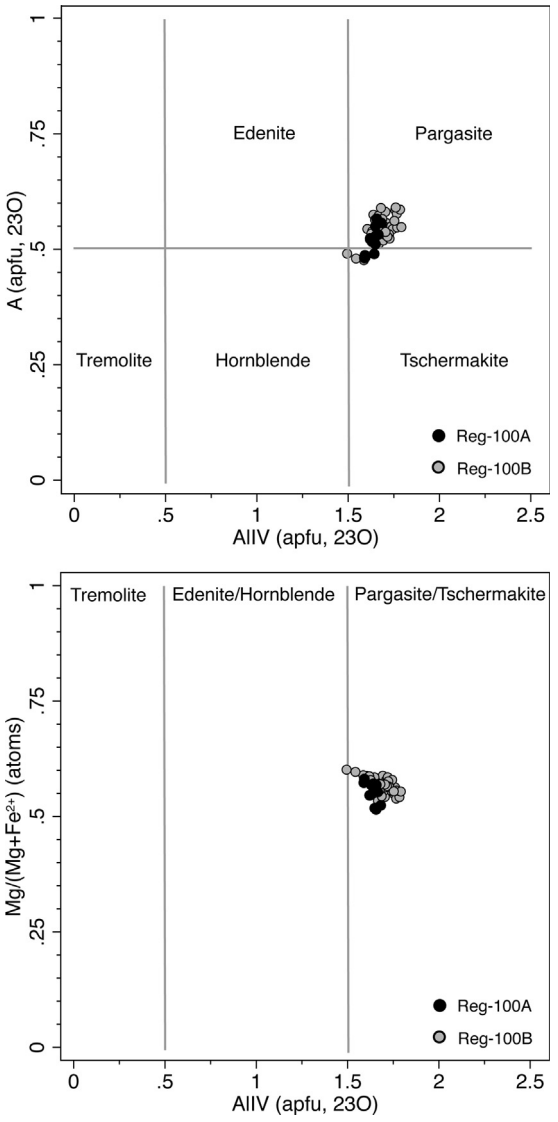

Fig. 5. Classification of amphibole in garnet amphibolites Reg-100A and Reg-100B.

The main mineral assemblage is locally overprinted by a post-kinematic chlorite + albite + ilmenite.

4.2. Mineral chemistry

Amphibole is mostly pargasite and minor tschermakite (Fig. 5) with 0.03–0.07 Ti, 1.47–1.77 apfu AlIV, 0.78–1.00 apfu AlVI, 0.48–0.59 apfu NaA + K and $Mg/(Mg + Fe^{2+})$ ratio ranging from 0.52 to 0.60. No systematic compositional differences were found in between amphibole poikiloblasts and matrix amphibole.

In sample Reg-100A, *garnet* has a relatively homogeneous composition, with ca. 62 mol.% Alm, 15 mol.% Pyp, 20 mol.% Grs and 6 mol.% Sps. In Reg-100B, the garnet composition presents ca. 60 mol.% Alm, 15 mol.% Pyp, 20 mol.% Grs, whereas the spessartine component is slightly more variable, ranging from 8 mol.% in grain cores to 4 mol.% at grain rims (Fig. 6).

Plagioclase shows an oligoclase composition, with 17–19 mol.% An in Reg-100A, whereas in Reg-100B, it is albite–oligoclase, with 8–14 mol.% An.

Epidote from the foliated matrix shows X_{Fe3+} [$= Fe^{3+}/(Fe^{3+} + Al)$] values ranging from 0.19 in grain cores to 0.22 at the grain rims. X_{Fe3+} values in epidote grains included in garnet are close to 0.23.

Phengite shows ca. 3.11–3.20 apfu Si, and $Mg/(Mg + Fe^{2+})$ and Na/(Na + K) ratios ranging, respectively, from 0.36 to 0.48 and from 0.11 to 0.24. The coexisting *paragonite* presents a Na/(Na + K) ratio close to 0.90.

4.3. P–T conditions

In the garnet amphibolite, equilibrium temperature conditions for the Grt–Prg–Pl mineral assemblage were calculated using the Amp-Pl NaSi–CaAl exchange thermometer from Holland and Blundy (1994) that shows a precision of ± 40 °C at 1σ level. Pressures were estimated using two calibrations of the Amp–Pl–Grt–Qtz barometer from Kohn and Spear (1990; precision: ± 0.5 kbar) and the empirical Amp-Pl Si–Al partitioning barometer from Molina et al. (2015; precision ranges from ± 1.5 to ± 2.3 kbar).

The thermobarometric results and mineral compositions used in the calculations are listed in Table 2 in the electronic Supplementary Material. A total of nine amphibole–plagioclase–garnet compositional sets (six from sample Reg-100A and three from sample Reg-100B; only matrix amphibole and plagioclase, and garnet rims) were used in the calculations. Uncertainties in pressure and temperature estimates due to heterogeneities in mineral compositions are similar to or lower than those reported for the calibration of the thermobarometric expressions. Average isopleths of Amp–Pl NaSi–CaAl exchange, Amp–Pl Si-Al partitioning and Amp–Pl–Grt–Qtz equilibria for the two samples are displayed in Fig. 7A (see also Table 2 in the Supplementary Material). We consider the intersection of the average isopleths as the best estimate of the P-T conditions. The precision values of the calibrations indicated above were used for the uncertainties in the P-T estimates. For sample Reg-100B, the calculated *P–T* conditions using the various thermobarometric expressions are relatively close, clustering around 640–660 °C and 11–12 kbar. However, in sample Reg-100A, the temperature estimates show a larger range of variation reaching up to ca. 700 °C, whereas pressure estimates vary from 10 to 13 kbar.

5. Discussion

5.1. Phase relationships

The calculated *P–T* conditions for the mineral assemblage Grt–Prg–Pl from the garnet amphibolites from the Adrar–Souttouf Metamafic Complex are consistent with the stability fields of the mineral assemblages (Fig. 7B): (1) garnet + plagioclase in hydrous basalt compositions (Poli,

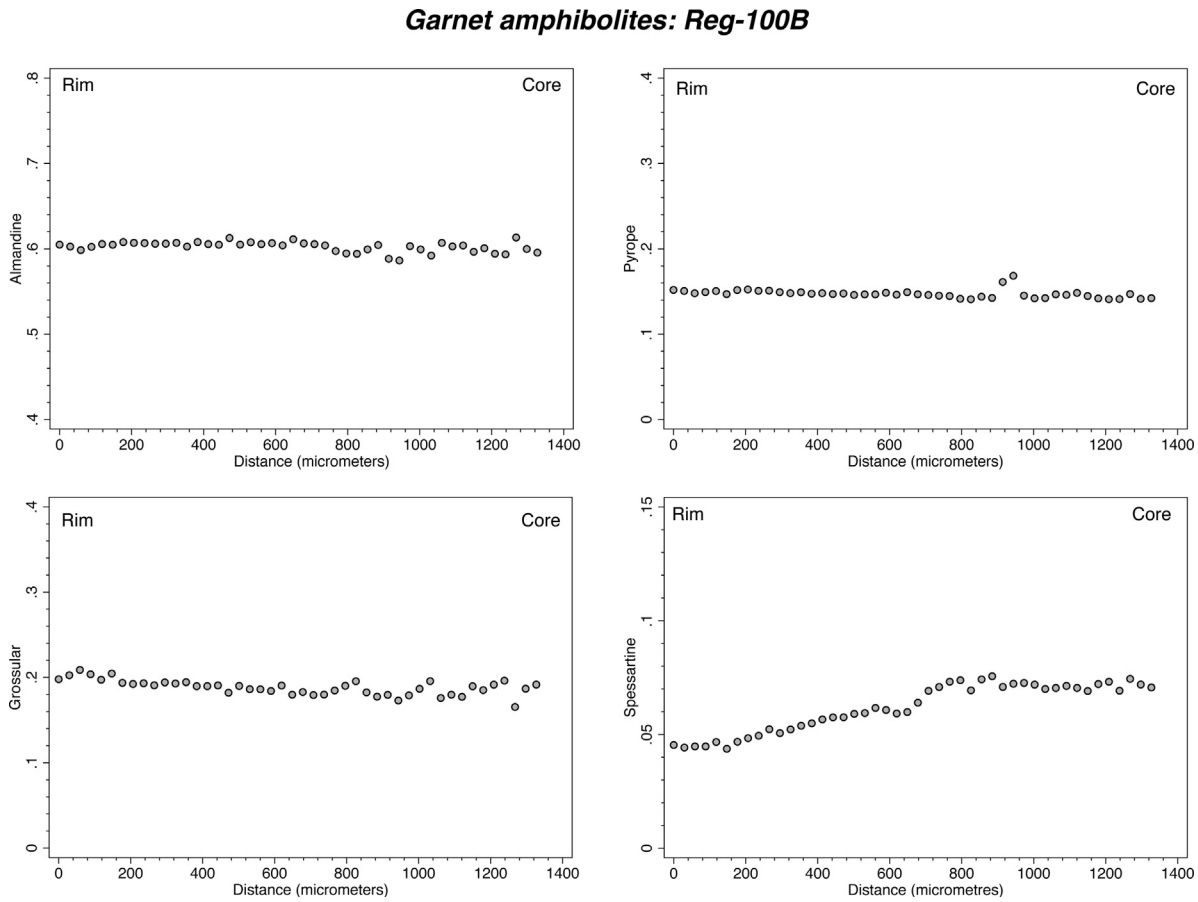

Fig. 6. Compositional profiles in garnet poikiloblast from garnet amphibolite Reg-100B.

1993), (2) paragonite + epidote + quartz + H_2O (Franz and Althaus, 1977), and (3) paragonite + quartz (Chatterjee, 1972; Holland, 1979). However, the estimated temperatures (Fig. 7B) are by 20–80 °C higher than wet-basalt solidus temperatures (e.g., Lambert and Wyllie, 1972; Wyllie and Wolf, 1993). Since there is no textural evidence of paragonite- and phengite-breakdown melting reactions, fluid-absent conditions or presence of a fluid phase with reduced H_2O activity were likely prevailing during metamorphism.

The pressures estimated for the mineral assemblage Grt–Prg–Pl are similar to those obtained for the paragonite-bearing garnet amphibolites from the Nevado–Filábride Complex, Betic Cordilleras, SE Spain, with the mineral assemblage garnet + barroisite + albite + paragonite + epidote + quartz + rutile + titanite (Molina and Poli, 1998) and from the Ise area of the Hida Mountains, Japan, which shows the mineral assemblage garnet + hornblende + epidote + paragonite + phengite + rutile +quartz (Tsujimori et al., 2006). However, temperature estimates are slightly higher, what can account for the presence of oligoclase instead of albite, a more common mineral phase in epidote–amphibolite facies (e.g., Molina and Poli, 1998). Temperature estimates are also higher than those calculated for the garnet amphibolites from the Boufkerine basement in Central Mauritanides (Caby and Kienast, 2009), which present a mineral assemblage consisting of barroisite + garnet + epidote + phengite + chlorite + quartz + rutile + ilmenite, formed at ca. 564 ± 23 °C and 10 ± 2 kbar.

On the other hand, pressure estimates for the garnet amphibolites from the northernmost end of the Adrar–Souttouf Metamafic Complex are lower than those calculated for eclogites from the Tarf Magneïna unit with the mineral assemblage garnet + omphacite (Jd_{30-40}) + barroisite + quartz+ rutile ± phengite + epidote that formed at 13–15 kbar and 550–600 °C (Le Goff et al., 2001). Several lines of evidence make it unlikely an early eclogite-facies metamorphic stage in the garnet amphibolites studied here. First, garnet grains from eclogites in the Tarf Magneïna unit present inclusions of omphacite and barroisite (Le Goff et al., 2001). By contrast, no relicts of such minerals exist in the garnets from the studied amphibolites. Second, the existence of symplectitic aggregates of clinopyroxene (Jd_{25-35}) + plagioclase ± quartz in the Tarf Magneïna unit eclogites is witness to garnet-omphacite-barroisite reactions (Le Goff et al., 2001). By contrast, no such aggregates are observed in the garnet amphibolites. Third, amphibole compositions in the

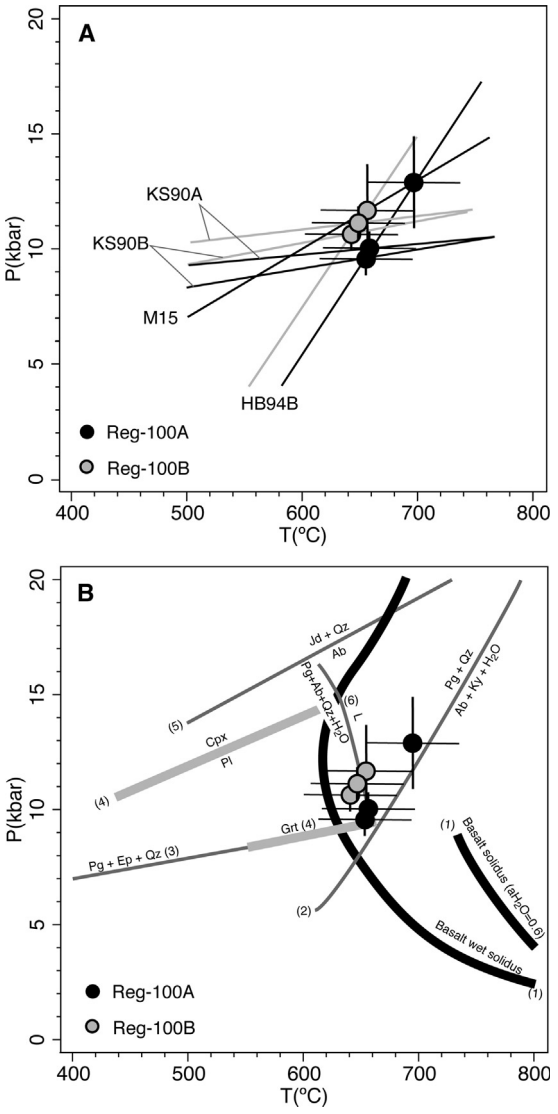

Fig. 7. A. *P–T* conditions for the Grt–Prg–Pl assemblage from the garnet amphibolites Reg-100A and Reg-100B estimated with the two calibrations of the Amp–Pl–Grt–Qtz barometer from Kohn and Spear (1990), the empirical Amp–Pl Si–Al partitioning barometer from Molina et al. (2015) and the Amp–Pl NaSi–CaAl exchange thermometer from Holland and Blundy (1994). Abbreviations: KS90A, calibration A of the Amp–Pl–Grt–Qtz barometer from Kohn and Spear (1990); KS90B, calibration B of the Amp–Pl–Grt–Qtz barometer from Kohn and Spear (1990); HB94B, calibration B of the Amp–Pl thermometer from Holland and Blundy (1994); M15, Amp–Pl barometer from Molina et al. (2015). See text for discussion. B. Reactions relevant to constrain the stability field of the Grt–Prg–Pl assemblage from the garnet amphibolites. Reactions: 1, Lambert and Wyllie (1972) and Wyllie and Wolf (1993); 2, Chatterjee (1972) and Holland (1979); 3, Franz and Althaus (1977); 4, Poli (1993); 5, Holland (1980); 6, García-Casco (2007). Mineral abbreviations after Whitney and Evans (2010).

two rock types are different, being mostly pargasite and minor tschermakite in the garnet amphibolite and barrosite in the eclogite. Furthermore, the latter also presents edenite and magnesio-katophorite at the reaction sites (Le Goff et al., 2001).

5.2. Geodynamic implications

Le Goff et al. (2001) dated the eclogite-facies metamorphism in the Tarf Magneïna unit at 333 ± 25 Ma (Sm–Nd garnet–omphacite geochronology). This led them to propose that the Tarf Magneïna unit was metamorphosed in a Variscan subduction zone active during the Late Devonian–Early Carboniferous times. This model contrasts however with the Neoproterozoic ages inferred for eclogite-facies metapelites (ca. 600 °C and > 12 kbar) in the Gadel Group in the central Mauritanides (Caby and Kienast, 2009). Therefore, there is no simple correlation between the northern and the central Mauritanides (see discussion in Le Goff et al., 2001, and Caby and Kienast, 2009).

Regarding the northernmost end of the Adrar–Souttouf Metamafic Complex, a Variscan age could be assumed for the high-P amphibolite-facies metamorphism based on the regional distribution of the main foliation (e.g., Michard et al., 2010, 2017, and references therein). That being the case, our new barometric results would suggest that the northernmost region of the Adrar–Souttouf Metamafic Complex was buried to shallower depths than the Tarf Magneïna unit further south. However, given the relatively high-temperature estimates that we obtained for the garnet amphibolites, a relation with the older, high-grade metamorphism cannot be disregarded. So, absolute radiometric dating of the high-pressure metamorphism in the studied area is needed to confirm these relationships.

6. Conclusions

Garnet amphibolites from the northernmost end of the Adrar–Souttouf Metamafic Complex present the main mineral assemblage garnet + low-Ti pargasite + oligoclase + phengite + epidote + quartz + rutile ± paragonite ± K-feldspar. Amphibole–plagioclase NaSi–CaAl exchange thermometry combined with garnet–amphibole–plagioclase–quartz and amphibole–plagioclase Si–Al partitioning barometry indicates that the main mineral assemblage was equilibrated at high-P amphibolite-facies conditions at 10–13 kbar and 650–700 °C.

The absence of evidence of anatexis in the amphibolites implies that the metamorphic reactions could more likely have proceeded under fluid-absent conditions or in the presence of a fluid phase with reduced H_2O activity, as paragonite and phengite remained stable.

Contrasting with the occurrence of eclogites in the Tarf Magneïna unit at the southern end of Oulad Dlim Massif, the absence of relicts of omphacite and its pseudomorphs in the garnet amphibolites studied here precludes the achievement of eclogite-facies conditions in the northernmost region of the Adrar–Souttouf Metamafic Complex. Therefore, this region may have been buried to shallower depths than the units further south, probably during the Variscan orogeny; however, precise absolute radiometric dating of the high-P amphibolite-facies metamorphism is required to confirm these findings.

Disclosure of interest

The authors declare that they have no competing interest.

Acknowledgements

The authors thank Lenka Baratoux and an anonymous referee for careful and thoughtful reviews, and Isabelle Manighetti and André Michard for editorial handling and comments. This work has been financed by the grants CGL2013-40785-P (Ministerio de Economía y Competitividad, Gobierno de España) and P12.RNM.2163 (Junta de Andalucía).

Appendix A. Supplementary data

Supplementary data associated with this article can be found, in the online version, at http://dx.doi.10.1016/j.crte.2018.05.005.

References

Arribas, A., 1968. El Precámbrico del Sahara español y sus relaciones con las series sedimentarias más modernas. Boletín Geológico y Minero de España 79, 445–480.

Bea, F., Montero, P., Haissen, F., El, A., rchi, A., 2013. 2.46 Ga kalsilite and nepheline syenites from the Awsard pluton, Reguibat Rise of the West African Craton. Morocco. Generation of extremely K-rich magmas at the Archean–Proterozoic transition. Precalien 1mbrian Res. 224, 242–254.

Bea, F., Montero, P., Haissen, F., Molina, J.F., Michard, A., Lazaro, C., Mouttaqui, A., Errami, A., Sadki, O., 2016. First evidence for Cambrian rift-related magmatism in the West African Craton Margin: the Derraman Peralkaline Felsic Complex. Gondwana Res. 423–438.

Bea, F., Montero, P., Haissen, F., Rjimati, E., Molina, J.F., Scarrow, J.H., 2014. Kalsilite-bearing plutonic rocks: the deep-seated Archean Awsard massif of the Reguibat Rise, South Morocco, West African Craton. Earth-Sci. Rev. 138, 1–24.

Caby, R., Kienast, J.R., 2009. Neoproterozoic and Hercynian metamorphic events in the Central Mauritanides: implications for the geodynamic evolution of West Africa. J. Afric. Earth Sci. 53, 122–136.

Chatterjee, N.D., 1972. The upper stability limit of the assemblage paragonite + quartz and its natural occurrences. Contributions to Mineralogy and Petrolgoy 34, 288–303.

Dale, J., Powell, R., White, L., Elmer, F.L., Holland, T.J.B., 2005. A thermodynamic model for Ca–Na–amphiboles in Na_2O–CaO–FeO–MgO–Al_2O_3–SiO_2_H_2O–O for petrological calculations. J. Metamorphic Geology 23, 771–791.

Dosso, L., Vidal, P., Sichler, B., Bonifay, A., 1979. Âge précambrien de dolérites de la dorsale Réguibat (Mauritanie). C. R. Geoscience 288, 427–430.

Ennih, N., Liégeois, J.-P., 2008. The boundaries of the West African Craton, with special reference to the basement of the Moroccan metacratonic Anti-Atlas belt. In: Ennih, N., Liégeois, J.-P. (Eds.), The Boundaries of the West African Craton, 297pp. 1–17 (Geol. Soc. Lond. Spec. Publ.).

Fabre, J., 2005. Géologie du Sahara occidental et central. Série/Reeks: Tervuren African Geosciences Collection. MRAC Tervuren, Belgique, 572 p.

Franz, G., Althaus, E., 1977. The stability relations of the paragenesis paragonite–zoisite–quartz. Neues Jahrbuch für Mineralogie, Abhandlungen 130, 159–167.

García-Casco, A., 2007. Magmatic paragonite in trondhjemites from the Sierra del Convento mélange. Cuba. Amer. Mineral. 92, 1232–1237.

Gärtner, A., Villeneuve, M., Linnemann, U., El Archi, A., Bellon, H., 2013. An exotic terrane of Laurussian affinity in the Mauritanides and Souttoufides (Moroccan Sahara). Gondwana Res. 24, 687–699.

Gärtner, A., Villeneuve, M., Linneman, U., Gerdes, A., Youbi, N., Guillou, O., Rjimati, E., 2016. History of the West African Neoproterozoic Ocean: key to the geotectonic history of Circum-Atlantic Peri-Gondwana (Adrar Souttouf West Africa, Moroccan Sahara). Gondwana Res. 29, 220–233.

Holland, T.J.B., 1979. Experimental determination of the reaction paragonite = jadeite + kyanite + H_2O and internally consistent thermodynamic data for part of the system Na_2O–Al_2O_3–SiO_2_H_2O with application to eclogites and blueschists. Contributions to Mineralogy and Petrology 68, 293–301.

Holland, T.J.B., 1980. The reaction albite = jadeite + quartz determined experimentally in the range 600-1200 °C. Am. Mineral. 65, 129–134.

Holland, T., Blundy, J., 1994. Non-ideal interactions in calcic amphiboles and their bearing on amphibole-plagioclase thermometry. Contributions to Mineralogy and Petrology 116, 433–447.

Jessell, M.W., Santoul, J., Baratoux, L., Youbi, N., Ernst, R.E., Metelka, V., Miller, J., Perrouty, S., 2015. An updated map of West African mafic dykes. J. Afric. Earth Sci. 112, Part B, 440–450.

Kohn, M.J., Spear, F.S., 1990. Two new barometers for garnet amphibolites with applications to southeastern Vermont. Am. Mineral. 75, 89–96.

Lambert, I.B., Wyllie, P.J., 1972. Melting of gabbro (quartz eclogite) with excess water to 35 kilobars, with geological applications. J. Geol. 80, 693–708.

Lécorché, J.-P., Bronner, G., Dallmeyer, R.D., Rocci, G., Roussel, J., 1991. The Mauritanide orogen and its northern extension. In: Dallmeyer, R.D., Lécorché, J.-P. (Eds.), The West African Orogens and Circum-Atlantic Correlations. Springer Verlag, Berlin, pp. 175–215.

Le Goff, E., Guerrot, C., Maurin, G., Johan, V., Tegyey, M., Ben Zarga, M., 2001. Découvertes d'éclogites hercyniennes dans la chaîne septentrionale des Mauritanides (Afrique de l'Ouest). C. R. Acad. Sci. Paris, Ser. IIa 333, 711–718.

Michard, A., Hoepffner, C., Soulaimani, A., Baidder, L., 2008. The Variscan Belt. In: Michard, A., Saddiqi, O., Chalouan, A., Frizon de Lamotte, D. (Eds.), Continental Evolution: the Geology of Morocco. Lecture Notes in Earth Sciences, 116, pp. 65–131.

Michard, A., Soulaimani, A., Hoepffner, C., Ouanaimi, H., Baidder, L., Rjimati, E.C., Saddiqi, O., 2010. The south-western branch of the Variscan Belt: evidence from Morocco. Tectonophysics 492, 1–24.

Michard, A., Saddiqi, O., Missenard, Y., Oukassou, M., Barbarand, Y., 2017. Les grandes régions géologiques du Maroc; diversité et soulèvement d'ensemble. Geologues 194, 4–12.

Molina, J.F., Moreno, J.A., Castro, A., Rodríguez, C., Fershtater, G.B., 2015. Calcic amphibole thermobarometry in metamorphic and igneous rocks: new calibrations based on plagioclase/amphibole Al-Si partitioning and amphibole/liquid Mg partitioning. Lithos 232, 286–305.

Molina, J.F., Poli, S., 1998. Singular equilibria in paragonite blueschists, amphibolites and eclogites. J. Petrol. 39, 1325–1346.

Montero, P., Bea, F., Haissen, F., Molina, J.F., González-Lodeiro, F., Mouttaqi, A., Errami, A., 2017. Dorsale Reguibat et Massif des Oulad Dlim, l'avancée des connaissances. Geologues 194, 37–46.

Montero, P., Haissen, F., El Archi, A., Rjimati, E., Bea, F., 2014. Timing of Archean crust formation and cratonization in the Awsard–Tichla zone of the NW Reguibat Rise, West African Craton. A SHRIMP, Nd–Sr isotopes, and geochemical reconnaissance study. Precambrian Res. 242, 112–137.

Montero, P., Haissen, F., Mouttaqi, A., Molina, J.F., Errami, A., Sadki, O., Cambeses, A., Bea, F., 2016. Contrasting SHRIMP U–Pb zircon ages of two carbonatite complexes from the peri-cratonic terranes of the Reguibat Shield: Implications for the lateral extension of the West African Craton. Gondwana Res. 38, 238–250.

Poli, S., 1993. The amphibole–eclogite transformation, an experimental study on basalt. Amer. J. Sci. 293, 1061–1107.

Rjimati, E.C., Michard, A., Saddiqi, O., 2011. Anti-Atlas occidental et Provinces sahariennes. In: Michard, A., et, al. (Eds.), Nouveaux Guides géologiques et miniers du Maroc, vol.6, 561pp. 9–95 (Notes et Mem. Serv. Geol. Maroc).

Rjimati, E., Zemmouri, A., 2002. Mémoire explicatif de la carte géologique du Maroc, feuille d'Awsard. Notes et Mem. Serv. Geol; Maroc 439 bis 439 bis, 1–38.

Schofield, D.I., Horstwood, M.S.A., Pitfield, P.E.J., Crowley, Q.G., Wilkinson, A.F., Sidaty, H.C.O., 2006. Timing and kinematics of Eburnean tectonics in the central Reguibat Shield, Mauritania. J. Geol. Soc. 163, 549–560.

Sougy, J., 1962a. Contribution à l'étude géologique des guelb Bou Leriah (Region d'Aoucert Sahara Espagnol). Bull. Soc. geol. France 7, 436–455.

Sougy, J., 1962b. West African Fold Belt. Geol. Soc. Amer. Bull. 73, 871.

Tsujimori, T., Liou, J.G., Ernst, W.G., Itaya, T., 2006. Triassic paragonite-and garnet-bearing epidote-amphibolite from the Hida Mountains, Japan. Gondwana Res. 9, 167–175.

Villeneuve, M., Bellon, H., El Archi, A., Sahabi, M., Rehault, J.-P., Olivet, J.-L., Aghzer, A.M., 2006. Evénements panafricains dans l'Adrar Souttouf (Sahara marocain). C. R. Geoscience 338, 359–367.

Villeneuve, M., Gärtner, A., Youbi, N., El Archi, A., Vernhet, E., Rjimati, E.-C., Linnemann, U., Bellon, H., Gerdes, A., Guillou, O., Corsini, M., Paquette, J.-L., 2015. The Southern and Central Parts of the "Souttoufide" Belt, Northwest Africa. J. Afric. Earth Sci. 112, 451–470.

Whitney, D.L., Evans, B.W., 2010. Abbreviations for names of rock-forming minerals. Am. Mineral. 95, 185–187.

Wyllie, P.J., Wolf, M.B., 1993. Amphibolite dehydration-melting: sorting out the solidus. In: Alabaster, P.H.M., Harris, N.B.W., Neary, C.R. (Eds.), Magmatic Processes and Plate Tectonics, 76Geological Society, London, pp. 405–416 (Spec. Publ.).

Youbi, N., Kouyate, D., Soderlund, U., Ernst, R.E., Soulaimani, A., Hafid, A., Ikenne, M., El Bahat, A., Bertrand, H., Rkha Chaham, K., Ben Abbou, M., Mortaji, A., El Ghorfi, M., Zouhair, M., El Janati, M., 2013. The 1750 Ma magmatic event of the West African Craton (Anti-Atlas Morocco). Precambrian Res. 236, 106–123.